Mécanique & Industries 5, 511–517 (2004)

DOI: 10.1051/meca:2004051

Mécanique & Industries

Experimental study and superplastic rheological characterization of Ti-6Al-4V

David Ollivier[a], Youssef Aoura, Abdelhak Ambari and Serge Boude

EMT, ENSAM CER d'Angers, 2 Bd du Ronceray, BP 3525, 49035 Angers Cedex, France

Received 4 December 2002, Accepted 6 February 2004

Abstract – The superplastic behaviour of a titanium alloy base Ti-6Al-4V during biaxial test was investigated. A numerical model using a finite element method is proposed to examine the superplastic deformation behaviour of an appropriate axisymmetric shaped part. An experimental procedure based on the measurement of the pressure applied and the height of the dome apex of the formed part, is used to identify the rheological parameters of the material behaviour law. This identification was carried out by comparisons between the results of simulation and experimentation relating to thickness, equivalent strain and stress. Three inflation tests were carried out at different equivalent strain rates (4×10^{-4}, 6×10^{-4} and 8×10^{-4} s^{-1}). This procedure is applied successfully to the forming of an industrial part. Indeed, this study henceforth allows one to predict thickness evolution in any point of an industrial part for an optimization of its uniformity.

Key words: Superplastic forming / Anand model / Ti alloy / Ti-6Al-4V / axisymmetric complex shape

Résumé – Étude expérimentale et caractérisation rhéologique superplastique du Ti-6Al-4V. Le comportement superplastique en déformation biaxiale de l'alliage à base de titane le Ti-6Al-4V, a été étudié. Un modèle numérique en éléments finis est proposé pour étudier le comportement superplastique d'une pièce à l'aide d'une matrice axisymétrique appropriée. Une procédure expérimentale basée sur la mesure de la pression appliquée et de la hauteur du dôme de la pièce formée, est utilisée pour identifier les paramètres rhéologiques de la loi de comportement du matériau. Cette identification est effectuée par des comparaisons entre les résultats de la simulation et ceux expérimentaux relatifs à l'épaisseur, la déformation et la contrainte équivalente. Trois essais de formage ont été effectués à des vitesses de déformation équivalentes différentes (4×10^{-4}, 6×10^{-4} et 8×10^{-4} s^{-1}). Cette procédure a été appliquée avec succès pour le formage d'une pièce industrielle. En effet, cette étude nous permet dorénavant de prévoir l'évolution de l'épaisseur en tout point d'une pièce industrielle, afin d'optimiser son uniformité.

Mots clés : Formage superplastique / modèle d'Anand / alliage de titane / Ti-6Al-4V / matrice axisymétrique complexe

1 Introduction

The superplastic forming process (SPF) of complex thin-sheet parts, is commonly used in the aerospace and automotive industry. This process induces in the blank very large strains under low stresses. Titanium alloy base Ti-6Al-4V is widely employed, due to its low density [1], its good mechanical behaviour in fatigue [2] and corrosion resistance at low temperatures ($T < 200$ °C). The forming process requires optimal conditions, as strain rate, temperature and grain size, which are to be determined for each material [1,3,4].

[a] Corresponding author:
david.ollivier@angers.ensam.fr

The finite element method analysis has been performed to predict the material behaviour during superplastic forming of thin sheets. The most common law used to characterize the viscoplastic material is [5–8]:

$$\sigma = K\,\dot{\varepsilon}^m \varepsilon^n \tag{1}$$

This Norton-Hoff law has the advantage of needing only three parameters to be identified. For titanium alloy base Ti-6Al-4V: the hardening effect is generally neglected ($n = 0$) if there is no grain growth [5,6,9,10]; the strain rate sensitivity of the stress exponent "m" is included between 0.5 and 0.9 [5,10,11] and the consistency "K", between 400 and 3500 MPa.s$^{\mathrm{m}}$ [5,10–12].

Notation

a	strain rate sensitivity of hardening or softening (dimensionless)
A	pre-exponential factor (s)
e	dome apex thickness (mm)
h_0	hardening constant (MPa)
i	number of strain rates considered (dimensionless)
j	number of strain – stress data for each strain rate j (dimensionless)
K	consistency coefficient of metal (MPa.s^m)
m	strain rate sensitivity of stress exponent (dimensionless)
n	hardening coefficient (dimensionless)
n'	strain rate sensitivity of saturation value (dimensionless)
ΔP	differential pressure applied on the blank
Q	activation energy (kJ.mole^{-1})
ρ	radius of curvature (mm)
S	Deformation resistance (MPa).
$\dot{S}$	Time derivative of deformation resistance (MPa.s^{-1})
$\hat{S}$	coefficient for deformation resistance saturation value (MPa)
S^*	Saturation value of deformation resistance (MPa)
T	Absolute temperature (K)
$\varepsilon_{\mathrm{eq}}$	equivalent strain
$\dot{\varepsilon}_{\mathrm{eq}}$	equivalent strain rate (s^{-1}).
ξ	multiplier of stress (dimensionless)
σ_{eq}	equivalent stress (MPa)
σ^{e}	experimental stress for the same stress level i and strain rate j (MPa)
σ^{P}	computational stress for the same stress level i and strain rate j (MPa)
w_{ij}	weighting function (dimensionless)

More complex models were developed to take into account other parameters of material behaviour. One will cite for example, the behaviour law developed by Zhou [13], which is adapted to this material at high temperature. The associated model takes into account diffusional creep, enlargement of the grains and grain boundary sliding. An identification of the rheological parameters of this law was carried out and validated for the Ti-6Al-4V at 927 °C in uniaxial test [13, 14].

The problem concerning this identification is the microscopic knowledge of the material: grains size and their evolution, quantification of the grain boundary sliding... In this paper, this microstructural concept of the material is not study. A phenomenological aspect is privileged. For all these reasons a phenomenologic law (Anand [15]) is retained in order to describe the behaviour of titanium alloy base Ti-6Al-4V.

2 Material and experimental procedure

Table 1 shows the analysed chemical composition of Ti-6Al-4V titanium alloy.

In the literature, the rheological parameters identification of a superplastic behaviour material is often carried out from traction tests [12, 13]. It does not reflect the material conditions used in industrial process, where it is manufactured in biaxial deformation. To approach these conditions, the characterization of material is then carried out by inflation tests using an appropriate axisymmetric die. The geometry of this die [8] (named "evolutive cone") is designed to keep constant stress and pressure during the deformation of the blank. During the phase where the blank is in contact with the die, the radius of curvature of his dome apex is controlled by the geometrical shape of this die. According to the membrane theory [16] as the blank is a thin shell and the radius of curvature is very large in front of thickness, the equivalent stress can be given by:

$$\sigma_{\mathrm{eq}} = \frac{\rho\, \Delta P}{2\, e} \tag{2}$$

Furthermore, the radius of curvature ρ depends on angle α of the conical die and the thickness e is controlled by the material characteristics (m and K). In this conditions, the angle α evolution of the die had been designed to keep a ratio $\frac{\rho(\alpha)}{e(m,K)}$constant. Then, at constant pressure of forming, we obtain a constant equivalent stress at the dome apex as the blank remain in contact with the die.

$$\frac{\sigma_{\mathrm{eq}}}{\Delta P} = \frac{\rho\,(\alpha)}{2.e\,(m,K)} = \text{constant} \tag{3}$$

Table 1. Chemical composition of the Ti-6Al-4V titanium alloy.

Alloy element	Al	V	Fe	O_2+2N_2	C	N2	H_2	Y	Ti
Mass	5.5 to 6.75%	3.5 to 4.5%	<0.3%	<0.25%	<0.08%	<0.03%	<80 ppm	<50 ppm	Balance

Fig. 1. Superplastic Forming/Diffusion Bonding (SPF/DB) press.

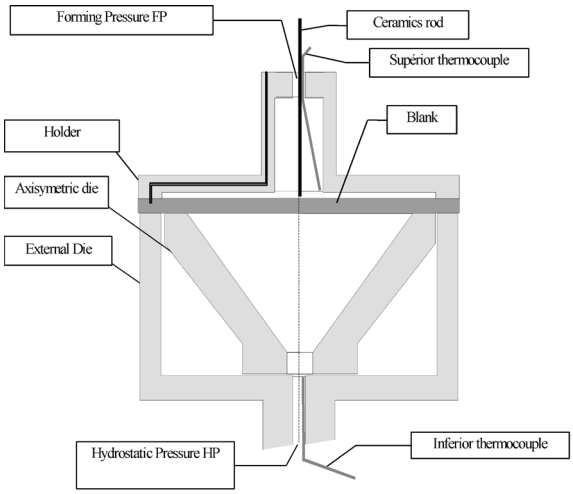

Fig. 2. SPF/DB schematics representation of experimental equipment.

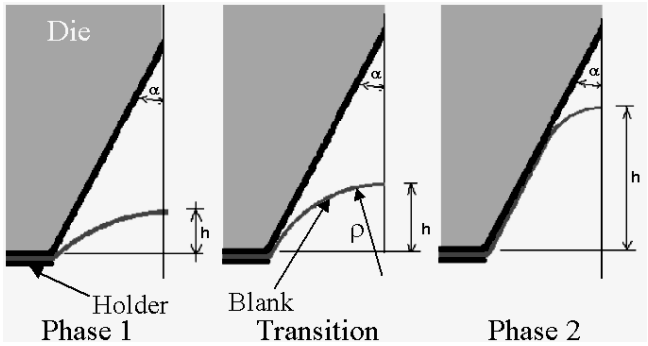

Fig. 3. Forming test with axisymetric die.

This relation permits us to calculate the equivalent stress from the measurements of the pressure, the radius of curvature and the thickness. The superplastic sheet forming is carried out on an instrumented press. We have developed a treatment method of experimental measurements which enables us to calculate equivalent stress σ_{eq} and equivalent strain rate $\dot{\varepsilon}_{\text{eq}}$, from the height of the part and the difference of the forming and the hydrostatic pressure ΔP applied to the blank.

The equipment (Fig. 1) permits the manufacture of parts, under argon pressure, with a diameter 200 mm and a depth of 200 mm. The maximum pressure applied can be 12 MPa at a temperature of 1300 °C. The development of a such press was carried out in our laboratory by Boude [7] and Boulos [8]. This one can form aluminium, titanium or nickel-based alloys.

The process unit manages three different pressures (Fig. 2): Forming Pressure FP applied on the upper face of the sheet; Hydrostatic Pressure HP applied on the lower face and Enclosure Pressure EP to reduce the creep phenomena in tools. For all tests the value of hydrostatic and enclosure pressure applied is fixed to 0.5 MPa.

The circular blank (Fig. 2) is maintained between the axisymmetric die and the holder die on its periphery tightening zone at the superplastic temperature domain of titanium alloy base Ti-6Al-4V ($T = 925$ °C). Inflation is carried out by argon pressurized on the side of the holder die. An inductive incremental position sensor (precision: 0.1 mm), associated to a ceramics rod, gives the height "h" at the dome apex. The height "h", the forming pressure FP, and the hydrostatic pressure HP, are recorded according to the time elapsed during forming.

Under the differential pressure $\Delta P = \text{FP} - \text{HP}$, the blank is gradually shaped on the die from a free spherical dome. During forming, the contact surface increases and the curvature radius at the dome apex decreases (Fig. 3).

The rheological parameters of the initial viscoplastic law (Eq. (1)) are determined beforehand for this material ($K = 492$ MPa.s^m and $m = 0.48$) in biaxial condition on the superplastic press described in Figure 2 [17]. From the calculation of equivalent stress, strain and strain rate, the rheological parameters of the Norton-Hoff law have been determined by using the least square method in the range of the strain rate studied (from 4×10^{-4} to 8×10^{-4} s^{-1}).

Three inflation tests were carried out at different equivalent strain rates (4×10^{-4}, 6×10^{-4} and 8×10^{-4} s^{-1}), the initial thickness of the blank being $e_0 = 1.2$ mm and the temperature of forming $T = 925$ °C. Differential pressure $\Delta P = \text{FP} - \text{HP}$, measured according to time, allow one to calculate the equivalent stress applied to sheet, from the Equation (2) [16].

3 Model and numerical simulation

3.1 Assumptions

a) The sheet material to be formed is supposed incompressible, homogeneous and isotropic [9, 18, 19].
b) The material is maintained at constant temperature during superplastic forming; incertitude on this one does not exceed 5 °C [8].
c) The structure is supposed stable: no phase change or of grain enlargement.
d) The consistency of the material K and the coefficient of sensitivity at strain rate m practically do not change with strain rate in the domain of material forming [5, 6, 11].
e) The strain hardening plasticity effect is ignored [5].
f) we take account of a constant friction coefficient at the interface between the sheet and die.

3.2 Identification of the Anand law parameters

The Anand law is used to describe the phenomena of viscoplastic flow in materials at high temperature [15]:

$$\dot{\varepsilon}_{\mathrm{eq}} = A \exp(-Q/RT) \left[\sinh\left(\frac{\sigma_{\mathrm{eq}}}{S}\right)\right]^{\frac{1}{m}} \tag{4}$$

with:

$$\dot{S} = \left(h_0 \left|B\right|^a \frac{B}{|B|}\right) \dot{\varepsilon}_{\mathrm{eq}} \tag{5}$$

where

$$B = 1 - \frac{S}{S^*} \quad \text{and} \quad S^* = \hat{S}. \left[\frac{\dot{\varepsilon}_{\mathrm{eq}}}{A} \exp(Q/RT)\right]^{n'}$$

We note:

$$H = A. \exp\left(-\frac{Q}{RT}\right) \tag{6}$$

The first step in the material characterization consists in the identification of the rheological parameters. The adopted assumption (e) permits one to deduce $a = 1$ and $n' = 0$. Moreover, as we assumed in hypothesis (c), the microstructural state of the material and the internal defects are stable, and so the parameter S representing the resistance to plastic flow is constant ($S = S^*$). Furthermore, the assumptions (b) permits to define the parameter H as constant. For the others, a mathematical development of the law is given in the case of constant strain rates. Thus, for a given strain rate the $\sigma_{\mathrm{eq}}(t)$ expression becomes:

$$\sigma_{\mathrm{eq}}(t) = \frac{S^*}{\xi}.\mathrm{Arc}\sinh\left[\left(\frac{\dot{\varepsilon}_{\mathrm{eq}}}{H}\right)^m\right] \tag{7}$$

The comparison of this relation (6) to Equation (1) gives a relationship between K and the Anand law parameters (Eq. (7)):

$$K = \frac{S^*}{\xi.H^m} \tag{8}$$

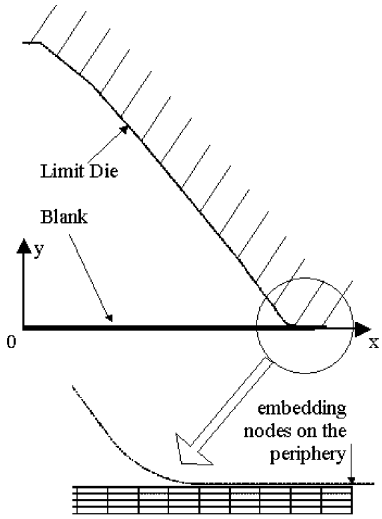

Fig. 4. Numerical forming process model.

The parameters of this law are identified by an optimisation procedure, using a weighted least-square method which minimizes the function f [14]:

$$f = \sum_{j=1}^{u} \sum_{i=1}^{v} w_{ij} \left[\left(\sigma_i^{\mathrm{P}}\right)_j - \left(\sigma_i^{\mathrm{e}}\right)_j\right]^2 \tag{9}$$

where w_{ij} is a weighting parameter for ith element ($0 \leq w_{ij} \leq 1$). For simplicity, we assume that w_{ij} is the same for all elements, which simplifies the multi-variable optimization problem into a single-variable problem. Equation (9) implies that the difference between the computed stress and the experimental one $\left[\left(\sigma_i^{\mathrm{P}}\right)_j - \left(\sigma_i^{\mathrm{e}}\right)_j\right]$ is minimized. The function f depends on the numbers of point (about 500 values of stress σ^{e} in experimental data base for each test). Concerning the computational stress σ^{P}, the numerical code permits to recover the same number of stress values of that experience.

3.3 Numerical simulation

Simulation, carried out with the finite element code "ANSYS", uses viscoplastic axisymmetric elements. The Anand law is used to describe the material behaviour. Boundary conditions are imposed to fix the blank on the periphery. The difference in inflation pressure $\Delta P = \mathrm{FP} - \mathrm{HP}$ is uniformly distributed on the blank (Fig. 4). Contact elements manage the large strains and the Coulomb friction coefficient witch are generated between the blank and the die. Friction is widely recognised as an important factor affecting the thinning of SPF components [1, 5, 7, 20, 21]. For this study, the friction coefficient is assumed to be constant and uniform along the contact surface (assumption f). Several cases were tested for different Coulomb friction coefficients witch varying from 0 to 1. The value selected for this coefficient is 0.2 (also retained by Bellet [5]). Indeed, this value permits to obtain the best thickness distributions of experimental products

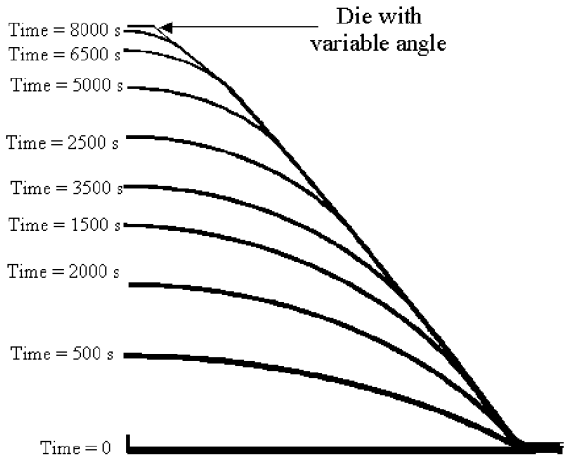

Fig. 5. Configurations of the deformed blank, for various time increment.

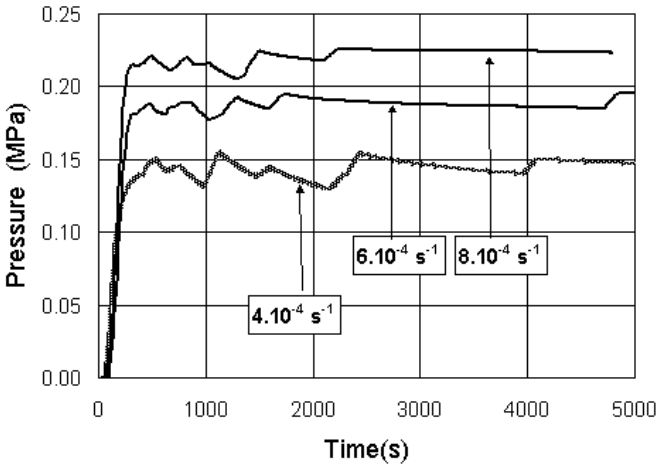

Fig. 6. Pressure applied on the blank for different equivalent strain rate $\dot{\varepsilon}_{\mathrm{eq}}$.

and the same final forming time. It is important to notice that the Coulomb friction coefficient is introduced at the level of the boundary conditions which are imposed in accordance with the experimental process. The determination of the rheological parameters is made for a chosen rheological law (Anand) and for the imposed boundary conditions. The simulated shape of the blank at various time increments is shown in Figure 5. One can note that the free dome is perfectly spherical and follows the assumption a.

4 Results and discussion

4.1 Experimental results

The differential pressure $\Delta P = \mathrm{FP} - \mathrm{HP}$ applied to the blank, measured according to time, is given in Figure 6. This one increases quickly toward a constant value. Once this imposed value is reached, the inflation of the blank is controlled by the conical shape of the axisymmetric die, designed to obtain a constant ratio $\frac{\Delta P}{\sigma}$. In Figure 6, the fluctuations in pressure are due to the servo control unit.

The thickness at the dome apex depends on the value of the coefficient m [7, 8]. It evolves according to the height (Fig. 7). However, it seems that the variation is independent on the strain rate in the range used for tests. The final part is given in Figure 8.

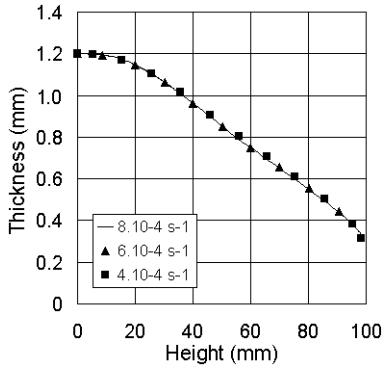

Fig. 7. Thickness at the dome apex evolution according to the time.

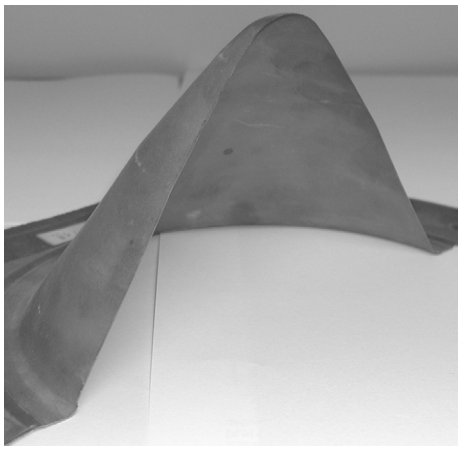

Fig. 8. Experimental part.

4.2 Simulation results and comparison

Figure 9 shows height evolution at the dome apex according to time, for three values of strain rate. The experimental results seem to be in good agreement with numerical simulations using Anand's law. The relative error on height ($\frac{h_{\mathrm{meseared}} - h_{\mathrm{simulated}}}{h_{\mathrm{meseared}}} * 100$) does not exceed 4.3%. This height evolution seems insensitive to the fluctuations of the pressure described previously (Fig. 6). This is due to the height inertia of the blank to the deformation.

The thickness at the dome apex measured at the end of the test is $e_{\mathrm{final}} = 0.36 \pm 0.01$ mm for the three formed parts. This one given by numerical simulation is $e_{\mathrm{final}} = 0.34$ mm. The relative error, varying from 2.9% to 8.8%, is finally in the range of the incertitude of experimental measurement. On the other hand, the equivalent strain at the dome apex determined by numerical

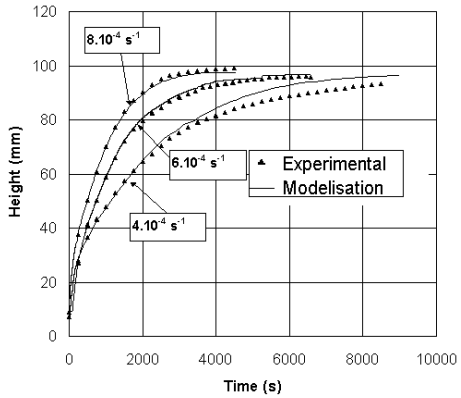

Fig. 9. Numerical et experimental results of dome height evolution according to the time.

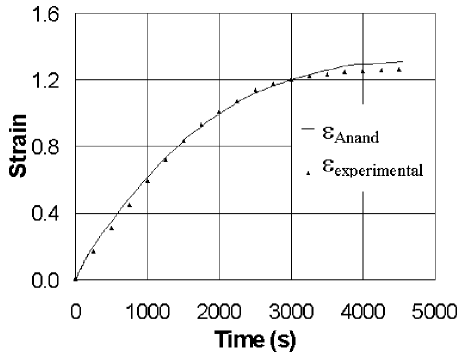

Fig. 10. Equivalent strain evolution at the dome apex, at equivalent strain rate $\dot{\varepsilon}_{eq} = 8 \times 10^{-4}$ s^{-1}.

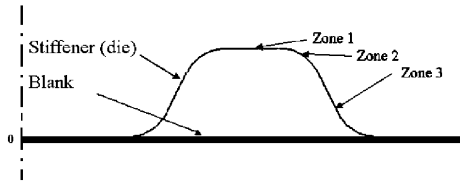

Fig. 11. Initial state of the blank on the die.

simulation using Anand's law provides good agreement with the experimental values. The relative error is lower than 3.2% (Fig. 10).

4.3 Utilisation of this procedure to the forming of an industrial part

To check the validity of this procedure, we apply it to the production of a industrial part with a more complex axisymmetric shape. The forming process uses a blank with an initial thickness equal to $e_0 = 1.1$ mm. It is meshed with four elements on the thickness. The Anand viscoplastic model, with its rheological parameters previously identified, is retained. The same Coulomb friction coefficient 0.2, is chosen. The blank is clamped on its periphery, as indicated in Figure 11.

The thickness comparison between numerical simulation and experimental data is shown in Figure 12. The

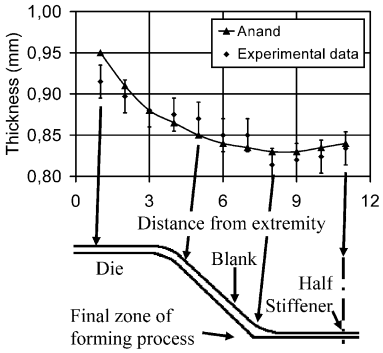

Fig. 12. Comparison of thickness distribution of the industrial part between simulated predictions and experimental measurements.

measured thickness remains largely in agreement with the numerical model, taking into account uncertainties of experimental measurements. The maximum difference between the experimental and the simulation final thickness is 0.035 mm located close to the embedding of the blank. The good agreement of the radius of curvature reached at the end of the forming, between the numerical simulation (R_s: 10 ± 0.5 mm) and experimental one (R_e: 9.5 ± 0.5 mm), is confirmed in zone 2 (Fig. 11).

5 Conclusion

The characterization method of titanium alloys base (Ti-6Al-4V) material makes it possible to increase the reliability of numerical simulations, for the prediction of the blank behaviour during the process, especially for industrial parts with complex shapes.

The experimental measures of the differential pressure and the height of the axisymmetric blank dome apex are used to identify the viscoplastic Anand rheological parameters. The identification of these parameters allows a good numerical description of the superplastic forming parts realized with equivalent strain rates going from 4×10^{-4} s^{-1} to 8×10^{-4} s^{-1}. This good agreement is confirmed by:

- (i) a lower deviation than 4.3% between the simulation and experimental height evolution according to the time,
- (ii) an absolute deviation from 0.01 to 0.03 mm for an initial thickness of 1.2 mm, between the simulated and experimental thickness obtained at the end of the forming,
- (iii) a maximum variation of 3.2% between the simulated and experimental strain, according to time.

The results obtained are well adapted to axisymmetric parts and titanium alloys base (Ti-6Al-4V) material. For more complex parts we need to use a large number of 3D elements to have a high degree of precision. In the future, it will be interesting to apply this method to other materials like aluminium alloys and to develop procedures to implement the Anand model with shell elements.

Acknowledgements. This study was funded by HUREL-HISPANO Le Havre under contract CIFRE (co-financed by French state). The authors gratefully acknowledge the monitors E. Szkolnik and M.-P. Bozec. The authors wish to thank P. Dal Santo for his generous assistance and helpful discussions.

References

[1] B. Baudelet, Mise en forme superplastique, Revue Française de mécanique n° 2 (1989)
[2] Y. Mutoh, M. Kobayashi, Y. Mae, T. Satoh, Fatigue properties of SPF/DB joints in titanium alloys, Superplasticity in Advanced Mater., S. Hori, M. Tokizane, N. Furushiro (ed.), The Japan Soc. For Research on superplasticity (1991) 405–410
[3] A.K. Ghosh, C.H. Hamilton, Mechanical behavior and hardening characteristics of a superplastic Ti-6Al-4V alloy, Metall. Trans. A 10 (1979) 699–706
[4] R. Grimes, R.G. Butler, The forming behavior of commercially available superplastic aluminium alloys, in: H.C. Heikkenen, T.R. Mcnelley (ed.), Superplasticity in Aerospace, The Metallurgical Society Inc. (1988) 97–114
[5] M. Bellet, Modélisation numérique du formage superplastique de tôles, Thèse, École nationale supérieure des mines de Paris, 1988
[6] Z. Chen, Z. Li, P. Dang, N. Chandra, Behavior of titanium alloy under uniaxial and biaxial superplastic conditions, Modelling the Mech. Response of structural Mater., E.M. Taleff, R.K. Mahidhana (ed.), The Minerals, Metals & Mater. Soc. (1997) 191–199
[7] S. Boude, Maîtrise du procédé de formage superplastique et réalisation d'une installation pilote, Thèse, École centrale de Nantes, 1994
[8] Z. Boulos, Interactions matériaux – procédé dans la mise en forme superplastique d'alliages réfractaires, Thèse, ENSAM d'Angers, 1999
[9] J.-P. Lechten, J.-C. Patrat, B. Baudelet, Analyses théorique et expérimentale du gonflement dans le domaine de superplasticité, Revue de Physique Appliquée 12 (1977) 7–14
[10] J.H. Chen, S. Lee, Methods for resolving Grooving Problems in Parts factored from combined Diffusion Bonding and Superplastic forming, J. Mat. Proc. Tech. (1994) 249
[11] K.S. Lee, H. Huh, finite element simulation of superplastic punch forming with a thickness control ring, J. Mater. Process. Technol. 63 (1997) 684–689
[12] W.C. Zhang, Wood, Zienkiewicz, Superplastic Forming using a Finite Element Viscous Flow Formulation, Inst. Metals 4 (1986) 1111
[13] M. Zhou, F.P.E. Dunne, Mechanisms-based constitutive equations for the superplastic behavior of a titanium alloy, J. Strain Analysis 31 (1996) 187–196
[14] J. Lin, J. Yang, GA-based multiple objective optimisation for determining viscoplastic constitutive equations for superplastic alloys, Int. J. Plasticity 15 (1999) 1181–1196
[15] L. Anand, Constitutive equations for the rate-dependent deformation of metals at elevated temperatures, J. Eng. Mater. and Techn. Trans. ASME 104(1) (1982) 12–17
[16] S. Timoshenko, Résistance des Matériaux 2^{e} partie, Librairie Polytechnique Ch. Béranger, 1954, pp. 142–143
[17] D. Ollivier, Le formage superplastique associé au soudage par diffusion appliqué à l'alliage à base de titane Ti-6Al-4V pour la fabrication de nacelles aéronautiques, Thèse, ENSAM d'Angers, 2003
[18] D.M. Woo, The analysis of axisymmetric forming of sheet metal and the hydrostatic bulging process, Int. J. Mech. Sci. 6 (1964) 303–317
[19] B. Storakers, Finite plastic deformation of a circular membrane under hydrostatic pressure, Int. J. Mech. Sci. 8 (1966) 619–628
[20] J.H. Cheng, The determination of material parameters from superplastic inflation tests, J. Mater Process Technol 58 (1996) 233–246
[21] Y. Chen, K. Kibble, R. Hall, X. Huang, Numerical analysis of superplastic blow forming of Ti–6Al–4V alloys, Materials & Design 22(8) (2001) 679–685